Journal of Physics and Chemistry of Solids 86 (2015) 114–121

Contents lists available at ScienceDirect

Journal of Physics and Chemistry of Solids

journal homepage: www.elsevier.com/locate/jpcs

Theoretical studies of the osmium based perovskites $AOsO_3$ (A=Ca, Sr and Ba)

Zahid Ali [a,b,*], Abdul Sattar [a,b], S. Jalali Asadabadi [c], Iftikhar Ahmad [a,b]

[a] Center for Computational Materials Science, University of Malakand, Chakdara, Dir (L), Pakistan
[b] Department of Physics, University of Malakand, Chakdara, Dir (L) Pakistan
[c] Department of Physics, Faculty of Science, University of Isfahan, Hezar Gerib Avenue, Isfahan 81744, Iran

ARTICLE INFO

Article history:
Received 9 March 2015
Received in revised form
18 June 2015
Accepted 3 July 2015
Available online 4 July 2015

Keywords:
Ceramics
Metals
ab-initio calculations
Electronic structure
Magnetic properties

ABSTRACT

Osmium based perovskites $AOsO_3$ (A=Ca, Sr and Ba) have been studied theoretically using density functional theory approach. These studies show that $CaOsO_3$ and $SrOsO_3$ are orthorhombic and $BaOsO_3$ is cubic and are consistent with the experiments. The electronic band structures demonstrate that these compounds are metals. The magnetic studies verify the experimental observations at low temperature, where the spin effects are canceled by the orbitals. The stable magnetic phase optimizations and magnetic susceptibilities calculations by the post-DFT treatment confirm that $CaOsO_3$ and $SrOsO_3$ are weak ferromagnetic whereas $BaOsO_3$ is a paramagnetic material. The directional magnetic study shows that these compounds are magnetically anisotropic, and reveals that the easy magnetization axis is [001] direction.

1. Introduction

Transition metals (TM) with 5d state compounds have recently attracted the focus of materials scientist due to their interesting behaviors of spin-orbit coupling (SOC) and electrons correlation effects, which strongly influences the electronic and magnetic properties of these compounds [1–6]. Magnetism in the 3d TM compounds is mainly originated from the spin moments of the d-electrons rather than the orbitals moment which is quenched by the crystal fields [7]. In contrast with the more familiar 3d Mott insulators, for which new physical phenomena originate from the onsite Coulomb interaction, in 5d TM oxides the electron correlation has been disputed to be driven by a large SOC [8–10].

The application of high pressure experimental techniques enabled researchers to synthesize and explore new perovskites, whose synthesis was not possible under ambient pressure [11] like $CaRuO_3$, $SrRuO_3$ and $BaRuO_3$. Magnetism in this series of compounds is a function of the ionic size of the Ca, Sr and Ba site cations [12]. Recently Shi et al. [13] synthesized a similar series of compounds with Ru replaced by Os ($CaOsO_3$, $SrOsO_3$ and $BaOsO_3$) and characterized the orthorhombic structure of these compounds with space group Pnma no. 62 except cubic $BaOsO_3$, using X-ray diffraction technique.

The electrical conductivity of these osmiumates shows that $CaOsO_3$ is not a good conductor as compared to $SrOsO_3$ and $BaOsO_3$. Zheng et al. [14] also reported that no energy gap is observed in the optical measurements of the cubic $BaOsO_3$. This behavior of $CaOsO_3$ is due to the tilting of the octahedra on the t_{2g} band width. In the temperature range 2–300 K, these compounds do not exhibit significant degree of magnetization upon cooling. The magnetic hysteresis has not been observed in these compounds and hence no long-range magnetic order has been observed [13]. Very recently Jung and Lee [15] investigated the electronic structure and magnetic properties of the cubic $BaOsO_3$ and few related compounds using ab-initio calculations. Though, these osmiumates perovskites are interesting systems because of their 5d states and need extensive theoretical and experimental studies to explore their physical properties especially spin orbit interaction and correlation effects which have not been addressed in details.

In the present work the full potential linearized augmented plane waves (FP-LAPW) method with Perdew–Burke–Ernzerhof generalized gradient approximation (GGA-PBE) including band correlated Hubbard and spin orbit coupling (GGA+U+SOC) along with BoltzTraP techniques are used to explore the physical properties of $CaOsO_3$, $SrOsO_3$ and $BaOsO_3$ compounds.

2. Computational details

Kohn–Sham equations [16] are solved, for the compounds under study, using the full potential linearized augmented plane

* Corresponding author at: Department of Physics, University of Malakand, Chakdara, Dir (L), Pakistan.
E-mail address: zahidf82@gmail.com (Z. Ali).

http://dx.doi.org/10.1016/j.jpcs.2015.07.001
0022-3697/

waves (FP-LAPW) method [17] with the GGA-PBE exchange correlation functionals [18] and GGA+U+SOC [19]. The electron density is obtained by summing over all the occupied states in Kohn–Sham equations [20]. The details about the spin dependent FP-LAPW method and the WIEN2k software used in these calculations are available in Ref. [21]. The potential used in the calculations is of the general form, where the core electrons are treated relativistically and the valance electrons are treated semi-relativistically. An approximated correction value is selected for U_{eff} =U–J, so that to get well corrected converged results after going through many values of Hubbard potential to adjust Os-5d density of states. For getting better results of the $AOsO_3$ compounds we used the GGA+U (SIC) method [19], where U_{eff} is taken U=2 eV and setting J=0. Semi-core states of the compounds are included with local orbitals so that no electron leakage can take place. To ascertain well converged and precise results $R_{MT} \times K_{MAX}$=7.5 basis functions are used. We have chosen the muffin–tin radii for Ca (2.2 a.u) Os (2.04 a.u), O (1.67 a.u) in $CaOsO_3$, for $BaOsO_3$, for Sr (2.43 a.u) Os (2.05 a.u), O (1.67 a.u) $SrOsO_3$ with $11 \times 7 \times 11$ k-mesh, and for Ba (2.5 a.u), Os (2.0 a.u), O (1.64 a.u) respectively and $10 \times 10 \times 10$ k-mesh are taken for these calculations.

To deal with the semi-classical transport coefficients of the compounds Boltztrap code package, developed by Madsen and Singh [22] based on Boltzmann transport theory is used. This code is found very successful in dealing with the transport properties of high temperature super conductors, thermoelectric materials and intermetallic compounds [23].

3. Results and discussions

3.1. Structural properties

In the present work the structural properties and geometries of the osmium based perovskites, $CaOsO_3$, $SrOsO_3$ and $BaOsO_3$, are investigated using density functional theory and analytical ionic radii methods. The unit cell of $CaOsO_3$ and $SrOsO_3$ are orthorhombic, while $BaOsO_3$ exists in cubic phase as shown in Fig. 1(a, b). The crystal structure of each compound is optimized; variation in energy versus change in volume curves for all the three compounds are shown in Fig. 2. The structural parameters like lattice constants, bulk moduli, ground state energies and volumes are evaluated with the use of the fitted Birch–Murnaghan equation of state [24] and are presented in Table 1. Furthermore, the mathematical expressions for the calculations of the lattice constants of the orthorhombic $CaOsO_3$ and $SrOsO_3$ perovskites using ionic radii are [25]

$$a = 1.515(r_A + r_o) + 1.312(r_B + r_o) - 0.866 \quad (1)$$

$$b = 0.083(r_A + r_O) + 2.102(r_B + r_O) + 1.115 \quad (2)$$

$$c = 1.626(r_A + r_o) + 2.471(r_B + r_o) - 1.208 \quad (3)$$

in the above equations, r_A is the ionic radius of A (A=Ca and Sr) with values of 0.99 Å and 1.12 Å respectively, r_B is the ionic radius of Os (0.63 Å) and r_o is the ionic radius of O and its value is 1.4 Å [26,27]. Similarly, the empirical formula for the calculations of the lattice constant of the cubic $BaOsO_3$ is [27]

$$a_o = \alpha + \beta(r_{Ba} + r_o) + \gamma(r_{Os} + r_o) \quad (4)$$

where α (0.06741), β (0.4905) and γ (1.2921) are constants and r_{Ba} is the ionic radius of Ba (1.35 Å).

The calculated data listed in Table 1 is obtained by both density functional GGA and analytical ionic radii techniques. In $CaOsO_3$ the lattice constants are 0.86%, under estimated by GGA approach and 0.06% over estimated by the analytical ionic radii technique, in $SrOsO_3$ the lattice constants are 0.52% under estimated through GGA and 0.52% over estimated by the ionic radii technique and in $BaOsO_3$ the lattice constant is 0.87% under estimated by GGA and 0.29% over estimated by the ionic radii technique. These results show the reliability of our calculated values and can be used as input variables for further studies without any hesitation.

The crystal structure of a perovskite compound can be estimated by its tolerance factor. Hence in the study of perovskite compounds, this parameter plays a key role in the determination of its structure. Tolerance factor can be calculated either by the ionic radii method (Eq. (5)) [25] or by the bonds length between different atoms in a compound using Goldschmidt formula [28] (Eq. (6))

$$t = \frac{(r_A + r_o)}{\sqrt{2}\,(r_B + r_o)} \quad (5)$$

$$t = \frac{(\langle A - O \rangle)}{\sqrt{2}\,(\langle B - O \rangle)} \quad (6)$$

where $\langle A - O \rangle$ and $\langle B - O \rangle$ represent the average bonds length of Ca–O [Sr–O] (Ba–O) and Os–O [Os–O] (Os–O) in $CaOsO_3$ [$SrOsO_3$]

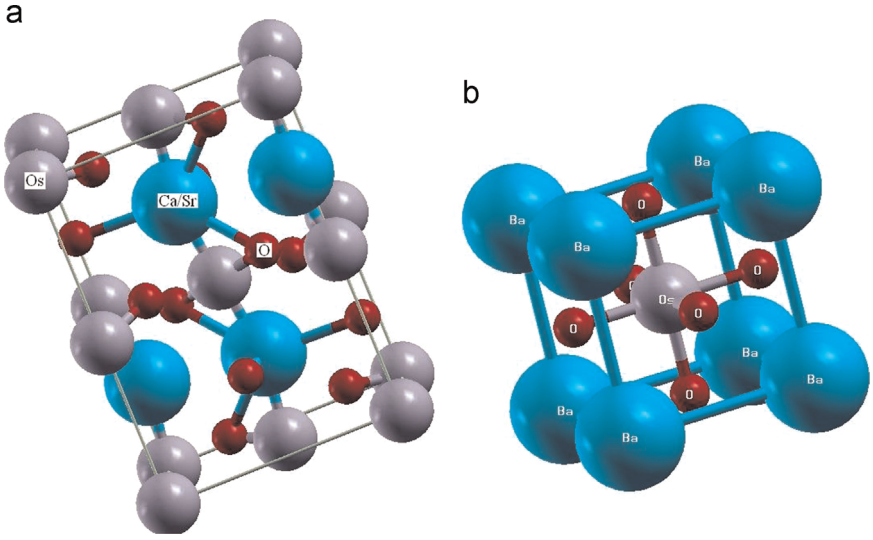

Fig. 1. Unit cell structures (a) orthorhombic $AOsO_3$ (A=Ca and Sr) and (b) cubic structure of $BaOsO_3$ perovskites.

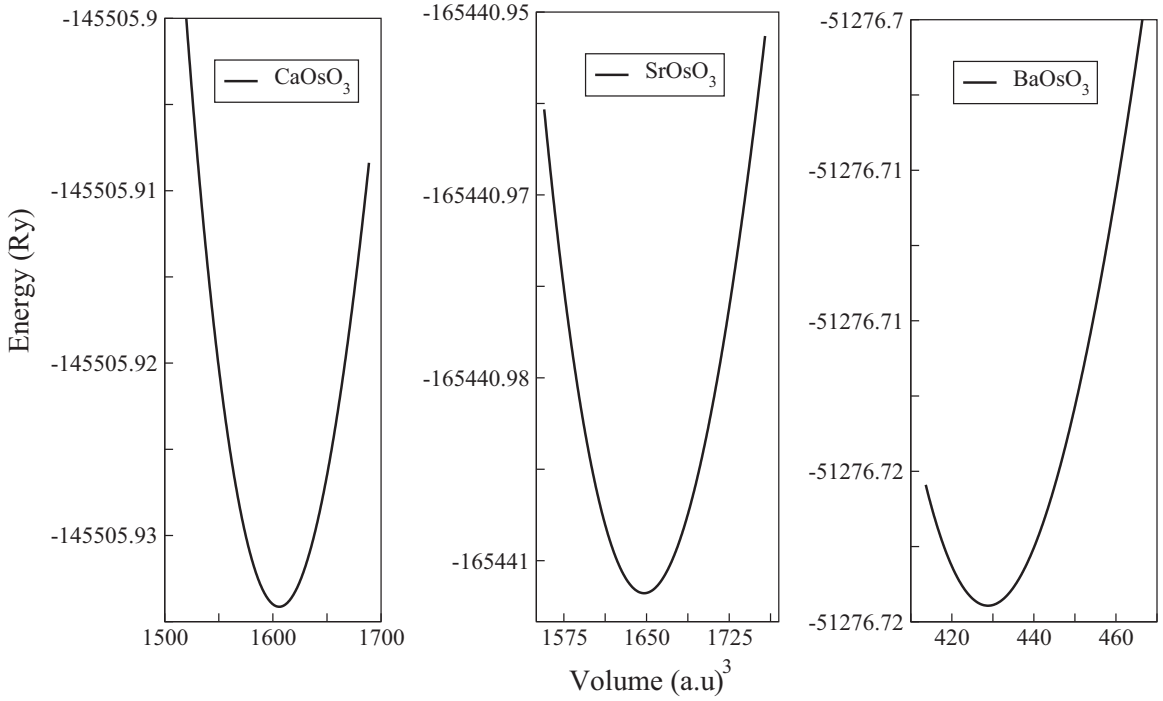

Fig. 2. Variation of optimal energy versus unit cell volume of $AOsO_3$ (A=Ca, Sr and Ba).

Table 1
Calculated and experimental lattice constants (a, b, c), volumes (V_0), bulk modulii (B), ground state energies (E_0), cohesive energies (E_{Coh}) difference between ferromagnetic, paramagnetic energies ($\Delta E = E_{FM} - E_{Para}$) and tolerance factor (t) of $AOsO_3$ (A=Ca, Sr and Ba) perovskites.

Compounds/ parameters	Present work (DFT)	Experimental Ref. [a]	Present analytical (ionic radii method)
$CaOsO_3$			
a (Å)	5.52614	5.57439	5.5779
b (Å)	7.70375	7.77067	7.6936
c (Å)	5.39828	5.44525	5.4140
V_0 (Å)^3	230.80352	235.87051	220.2447
B (GPa)	225.34293		
E_0 (eV)	−1979002.22		
E_{Coh}(eV)	−1520		
ΔE (eV)	−0.1292		
t	0.88	0.95	0.83
$SrOsO_3$			
a (Å)	5.53005	5.55925	5.5887
b (Å)	7.84630	7.88779	7.9049
c (Å)	5.56680	5.59802	5.6110
V_0 (Å)^3	244.18202	245.47428	241.5458
B (GPa)	208.8807		
E_0 (eV)	−2250940.33		
E_{Coh} (eV)	−953.8		
ΔE (eV)	−0.1224		
t	0.90	0.99	0.87
$BaOsO_3$			
a (Å)	3.9905	4.02573	4.0392
V_0 (Å)^3	63.54456	65.2430	
B (GPa)	205.0676		
E_0 (eV)	−697655.57		
E_{Coh} (eV)	−276.92		
ΔE (eV)	0.0165		
t	0.99	1.05	0.96

[13][a].

($BaOsO_3$). A compound with a tolerance factor in the range of 0.93–1.04 is cubic, [27,29] whereas for t greater than 1.04 the material is in hexagonal structure. Our calculated value for $BaOsO_3$ is 0.99 by DFT on the bases of bond lengths and 0.96 by the ionic radii method which confirm the cubic structure of the compound as the experimental value is little overestimated [13] which needs further experimental justifications, while the tolerance factor range for orthorhombic $CaOsO_3$ and $SrOsO_3$ is lesser than 0.93. Our calculated tolerance factor for $CaOsO_3$ is 0.88 by DFT and 0.83 by the ionic radii method, while similarly for $SrOsO_3$ are 0.90 and 0.87 respectively, presented in Table 1. Again the experimental values for both the compounds are overestimated. The tolerance factor lesser than 0.80 has usually ilmenite type structure ($FeTiO_3$) is more stable as compared to the perovskite structure. The change in bond lengths is responsible for the change in electronic and magnetic behavior of these compounds [30–32].

The charge distribution in an atom determines the nature of chemical bonding. The electronic charge density of a compound can be evaluated by the first-principle calculations, which is a very powerful theoretical tool for the explanation of the bonding nature between various atoms in a compound [31]. The 3-D electronic charge density of $AOsO_3$ (A=Ca, Sr and Ba) perovskite compounds for (100) and (110) planes are depicted in Fig. 3. The contours are drawn between −0.5 and 2 electrons/a.u.^{3} for all the three compounds. In the (100) plane of $AOsO_3$, O and A has almost spherical shape of the electronic cloud with no overlapping, justifies the ionic nature of bonding between these two elements, while in the (110) plane, Os and O transforms from spherical to almost dumbbell shape with an observable overlapping between Os and O exhibiting covalent bonding. The careful analysis of the electronic cloud of the other two compounds, $AOsO_3$ (A=Ca and Sr), the figure clearly indicates ionic bond between A (A=Ca and Sr) and O in the (110) plane, while in the (100) plane the electrons of the Os are overlapped with the oxygen electrons, demonstrating covalent bonding. The (100) planes of $CaOsO_3$ and $SrOsO_3$ show that there is metallic bonds exist between the Os atoms in both compounds.

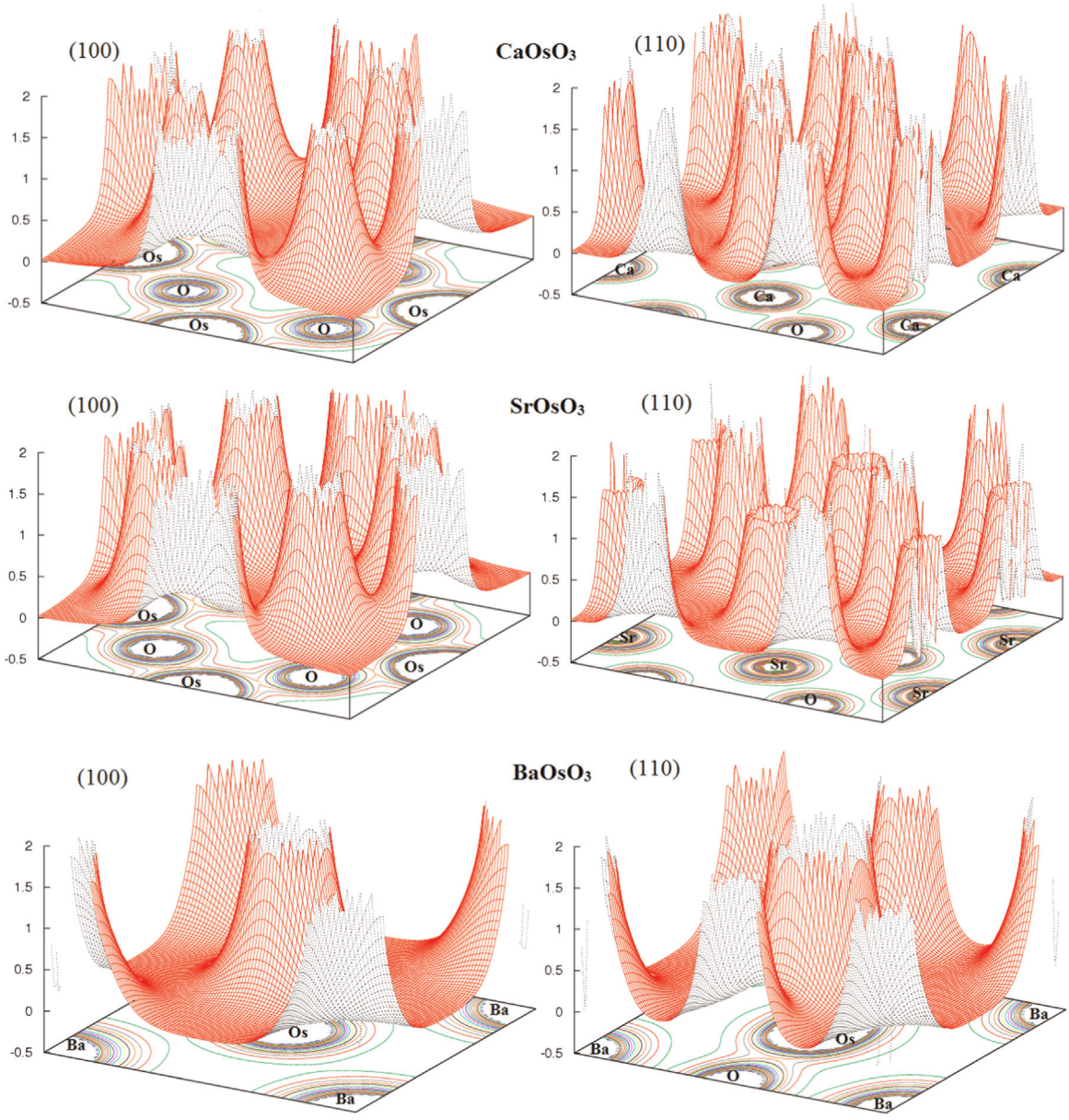

Fig. 3. 3-D counter plots of electronic charge densities of $BaOsO_3$, $CaOsO_3$ and $SrOsO_3$ in (100) and (110) planes (contours are drawn between −0.5 to 2 electrons/a.u.^{3}).

3.2. Cohesive energy

Cohesive energy is the energy required to split apart the constituent atoms of a substance into free atoms. According to Gaudoin et al. [33] cohesive energy is equal to the difference of the total energy of the compound and the energy of the individual free atoms. Though, the forces which are responsible for the cohesion process are Coulomb, magnetic and gravitational but the dominant contribution comes from Coulomb's interaction between charges in a compound. This energy plays pivotal role in the stability of a compound. Greater the magnitude of cohesive energy of a compound stronger will be its stability and vice versa [34]. In other words this energy is directly related to the strengths of bonds in a compound [35]. The cohesive energy for $AOsO_3$ (A=Ca, Sr and Ba) compounds are calculated using the well known equation of Dmitrii et al. [34]

$$E_{Coh} = E_{total} - (XE_{(A)} + YE_{(Os)} + ZE_{(O)}) \quad (7)$$

where E_{Coh} is the cohesive energy, E_{total} is the total energy of the compound that can be calculated from our GGA calculations, and X, Y, Z are constants representing the number of atoms in these compounds. For cubic perovskite $BaOsO_3$, $X=Y=1$ and $Z=3$, while for orthorhombic $AOsO_3$ (A=Ca and Sr), $X=Y=4$ and $Z=12$, where $E_{(A)}$, $E_{(Os)}$ and $E_{(O)}$ are the energies of free Ca, Sr, Ba, Os and O atoms respectively.

The calculated cohesive energies of the stated compounds listed in Table 1, show that $E_{Coh}(SrOsO_3) < E_{Coh}(CaOsO_3) < E_{Coh}(BaOsO_3)$. Hence $SrOsO_3$ is the most stable among the three compounds.

3.3. Electronic properties

Self consistent field (SCF) calculations are performed using GGA+U+SOC to investigate the electronic structure and magnetic behavior of $CaOsO_3$, $SrOsO_3$ and $BaOsO_3$ perovskites. The spin dependent electronic band profiles of these perovskites are presented in Fig. 4(a–c). It is clear from the plots that the valence and conduction bands, both in the spin up and down states, overlap with each other at the Fermi level making all the three compounds metallic. The calculated metallic nature of these compounds is in agreement with the experiments [13].

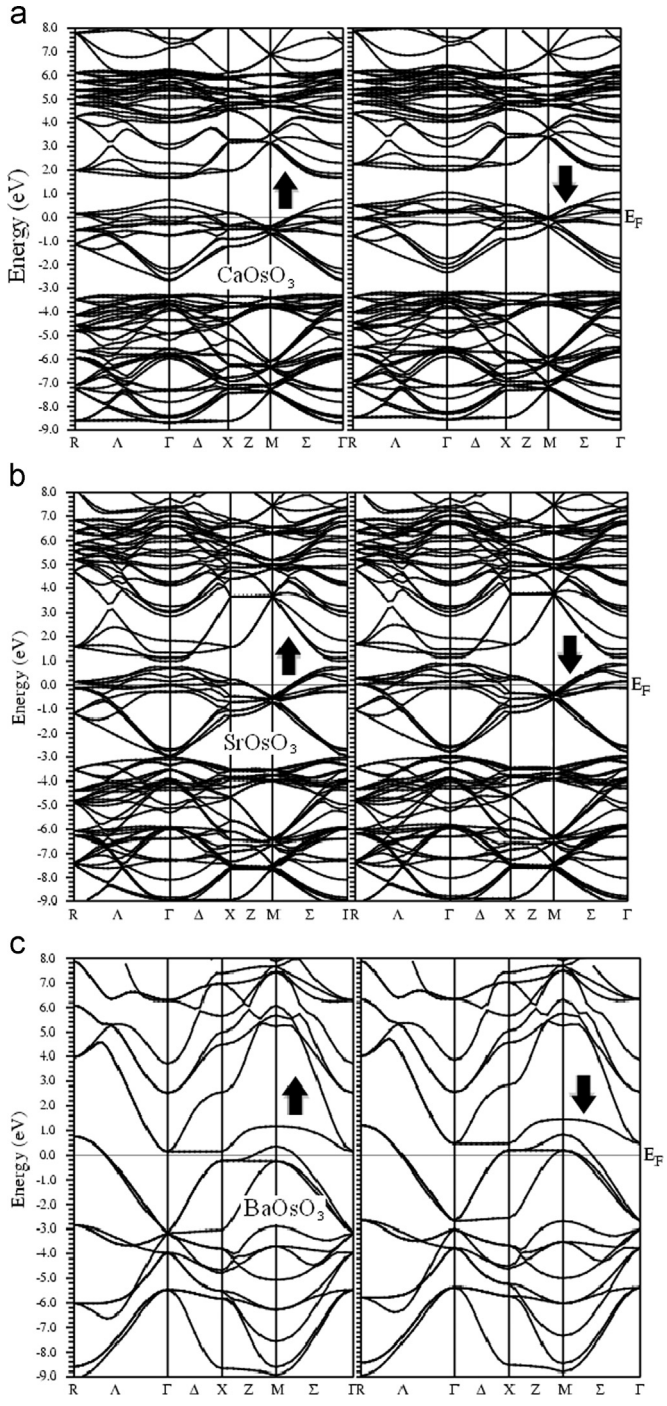

Fig. 4. Spin dependent band structure of (a) $CaOsO_3$, (b) $SrOsO_3$ and (c) $BaOsO_3$.

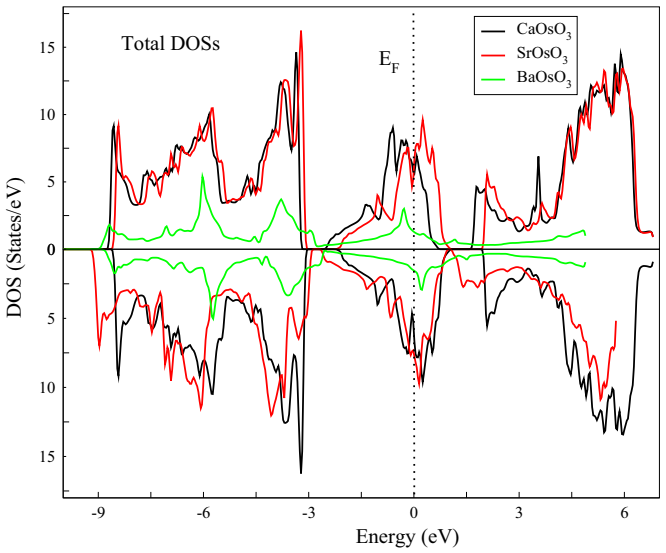

Fig. 5. Spin dependent total density of states of $AOsO_3$ (A=Ca, Sr and Ba).

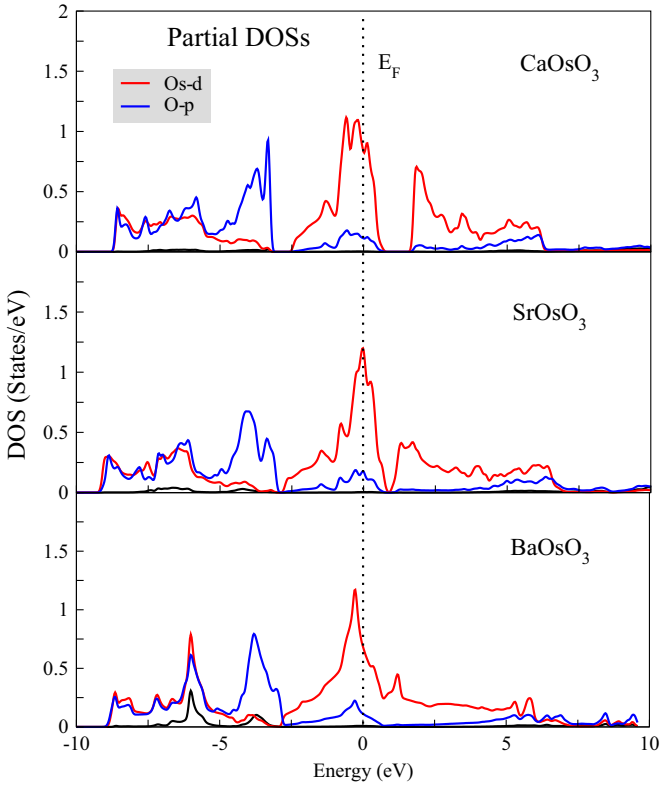

Fig. 6. Partial density of states of $AOsO_3$ (A=Ca, Sr and Ba).

To explain the origin of the spin dependent band structure of these compounds and contribution of different orbitals to the energy band structures, total and partial densities of states (DOS's) are calculated and shown in Figs. 5 and 6. It is clear from DOS plots that the electronic density for each compound is different in spin up and spins down states, demonstrating small polarization, where the DOS (states/eV) are more populated in the spin down states. It can be observed from Fig. 5 that the peaks of the top of the valance bands of $AOsO_3$ (A=Ca, Sr and Ba) occur at −3.3 eV and are extended towards higher energy level up to 2 eV in the conduction band. This extension of the states is responsible for the metallic behavior of these compounds.

The partial density of states shown in Fig. 6 reveals that the major contribution at the Fermi level is the strong hybridization of the O-2p states and Os-5d states makes these compounds metallic. The tiny polarization of the densities peaks towards the high energy level (Fermi level) exhibits magnetic instability in these compounds.

The electronic bands contribution at the Fermi level in these compounds, $AOsO_3$ (A=Ca, Sr and Ba), is mostly due to Os-5d but some contribution also comes from the O-2p states. The Os-5d triplet state, i.e. t_{2g} (d_{xy}, d_{yz}, d_{zx}), is winding as we go from Ca to Ba and this is the reason that $CaOsO_3$ is not as much conductive as the other two compounds. The comparatively nonconductive behavior of the $CaOsO_3$ is due to the tilting effect of the t_{2g} band's width [13].

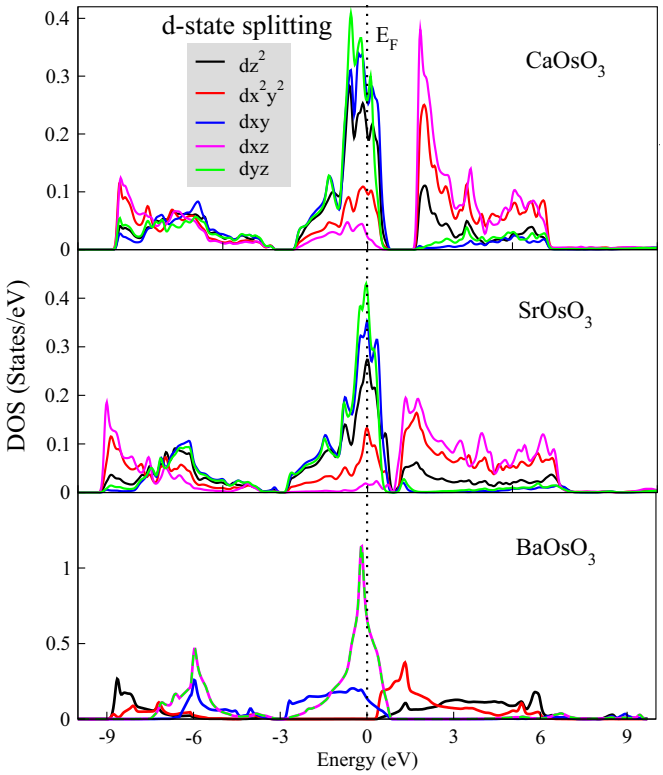

Fig. 7. d-state splitting of $AOsO_3$ (A=Ca, Sr and Ba).

Crystal fields in these compounds are responsible for the splitting of the degeneracy of the 5d-states of Os. These fields are generated by the Coulomb interaction between the 2p-state of oxygen and 5d-state of osmium in the OsO_6 octahedra, where the ligand oxygen interacts with the transition metal ion along the axis's. The crystal field splits the degenerate 5d-orbital of Os into non-degenerate doublet, e_g ($d_{x2-y2}+d_{z2}$), and triplet, t_{2g} ($d_{xy}+d_{yz}+d_{zx}$), states. Fig. 7 shows that the doublet state is higher in energy than the triplet state in $BaOsO_3$, while in the $CaOsO_3$ and $SrOsO_3$ the orthorhombic symmetry further leads to John Taller effect to remove the degeneracy of e_g and t_{2g} states. These states are further splitted in such a way that the e_g doublet state is splitted in to two levels (d_{x2-y2}, d_{z2}) and the t_{2g} triplet state is splitted in to three levels (d_{xy}, d_{yz}, d_{zx}).

The splitting process of the 5d-states of Os in these compounds under study is shown in Fig. 7. The plots demonstrate that the contribution in the energy in $AOsO_3$ (A=Ca and Sr) in the valance band ranges from −9 to −3 eV is due to d_{xz} state with some contribution from d_{xy} plus d_{xz} states. The Fermi level covers from −3 to 1 eV is contributed by d_{z2}, d_{xy}, d_{yz}, d_{x2y2} and d_{xy} but the maximum density at the Fermi level is contributed by d_{yz}, d_{xy} and dz^2 states of these compounds. In conduction band from 1 to 3 eV is mainly contributed by d_{xz} state and the top of the conduction band from 3 to 6 eV is also due to the d_{xz} state. The thick population at the Fermi level is due to d_{z2} and $d_{xy}+d_{yz}$ states, which makes $AOsO_3$ (A=Ca and Sr) compounds metallic. The contribution in the valance band of $BaOsO_3$ from −9 to −3 eV is due to the ($d_{z2}+d_{yz}$) e_g states, from −3 to 1 eV is mainly by t_{2g} ($d_{xy}+d_{yz}+d_{zx}$) states, while the contribution in the conduction band is due to ($d_{z2}+d_{x2y2}$) e_g states.

3.4. Magnetic properties

The magnetic properties of $CaOsO_3$, $SrOsO_3$ and $BaOsO_3$ compounds are investigated to examine the overall magnetic nature of these compounds and also check the contribution of electrons spin and orbitals motion to the net magnetic moments of the compounds. First of all the unit cells of all the three compounds are optimized for paramagnetic (non-magnetic) and ferromagnetic phases in order to verify the stable magnetic phase of each compound. The calculated energies difference between ferromagnetic and paramagnetic ($\Delta E=E_{FM}-E_{Para}$) phases are presented in Table 1. It is observed that the energy of the ferromagnetic phase of $CaOsO_3$ and $SrOsO_3$ is lower than their paramagnetic energies, while in $BaOsO_3$ the paramagnetic phase has lower energy than the ferromagnetic phase. These theoretical observations are in agreement with the experimental results [13]. Paramagnetism in compounds arises due to the unpaired electrons with no long range order. Paramagnetism is classified into two types, one is due to the localized electrons and the other is due to itinerant electrons which in other words is called Pauli-paramagnetism. Whereas ferromagnetism in perovskites is explained on the basis of indirect exchange interactions [27] in which double exchange favors in most cases ferromagnetism.

The spin magnetic moments, orbital magnetic moments and total magnetic moments of the compounds are calculated with the spin orbit coupling (SOC) technique in [001], [010] and [100] directions, in the interstitial as well as in the muffin tin sphere of $CaOsO_3$, $SrOsO_3$ and $BaOsO_3$ compounds. In these compounds Os has the main contribution in the magnetic properties, whereas the remaining atoms like A (A=Ca, Sr and Ba) and O have negligible effects so we ignore it. The calculated values of the magnetic moments are presented in Table 2. It is clear from the table that the positive values of the interstitial sites and orbitals moments reveal that these moments are parallel, while spin magnetic moments are negative showing anti parallel character for all the three compounds. The interstitial magnetic moments are 0.366 μ_B, 0.216 μ_B and 0.088 μ_B for $CaOsO_3$, $SrOsO_3$ and $BaOsO_3$ compounds respectively. The spin magnetic moments of Os in these compounds in (001) direction are −0.323 μ_B, −0.361 μ_B and −0.371 μ_B whereas the orbital moments are 0.325 μ_B, 0.364 μ_B and 0.357 μ_B respectively. Finally total spin and total orbital magnetic moments of each compound is calculated such that the total spin and total orbital magnetic moments of $CaOsO_3$ are −1.29 μ_B and 1.30 μ_B, while for $SrOsO_3$ it is −1.44 μ_B and 1.46 μ_B and for $BaOsO_3$ are −0.371 μ_B and 0.337 μ_B respectively. These moments combined to form net magnetic moments of a material. The total magnetic moment of $CaOsO_3$, $SrOsO_3$ and $BaOsO_3$ compounds are 0.376 μ_B, 0.236 μ_B and 0.074 μ_B respectively. Similarly in other directions like [010] and [100] the calculated values the orbital and spin magnetic moments of Os in $CaOsO_3$ are 0.282 μ_B, −0.298 μ_B, and

Table 2
Calculated interstitial (Int.), orbital (Orb.), spin and total magnetic moments of $AOSO_3$ (A=Ca, Sr and Ba) compounds expressed in the units of Bohr magnetron (μ_B) in [001], [010] and [100] directions.

Magnetic moments	$CaOsO_3$	$SrOsO_3$	$BaOsO_3$
[001]			
Int.	0.366	0.216	0.088
Spin (Os)	−0.323 × (4)	−0.361 × (4)	−0.371 × (1)
Orb.(Os)	0.325 × (4)	0.364 × (4)	0.357 × (1)
Tot.-spin	−1.290	−1.440	−0.371
Tot.-orb.	1.300	1.460	0.337
Tot.	0.376	0.236	0.074
[010]			
Orb.(Os)	0.282 × (4)	0.239 × (4)	0.313 × (1)
Spin (Os)	−0.298 × (4)	−0.312 × (4)	−0.271 × (1)
[100]			
Orb.(Os)	0.303 × (4)	0.249 × (4)	0.314 × (1)
Spin (Os)	−0.301 × (4)	−0.313 × (4)	−0.274 × (1)

0.303 μ_B, −0.301 μ_B for $SrOsO_3$ 0.239 μ_B, −0.312 μ_B and 0.249 μ_B, −0.313 μ_B and for $BaOsO_3$ 0.313 μ_B, −0.271 μ_B and 0.314 μ_B, −0.274 μ_B respectively. These results reveal that magnetic anisotropy exist in these compounds and show that the easy axis of magnetization is [001] direction. Our calculated results are consistent with the experimental work in which these materials do not show significant magnetization at low temperature from 2 K to 300 K and magnetic hysteresis was not obvious [13]. Similar behavior is also observed in our DFT calculations, as the orbital magnetic moments cancel the spins effects; results negligible moments. Hence our results are in conformity with the experiments.

Magnetic susceptibility (χ) plays important role to explain the magnetic order of a material. It is inversely related to temperature and with the increase in temperature thermal agitation increases and hence the disalignment of the magnetic moments takes place and consequently decreases the magnetic behavior of the compound [36,37]. Magnetism in materials can be understood by Curie Weiss law [36]. The Weiss constant (θ) is positive for ferromagnetic material, zero for paramagnetic and negative for anti-ferromagnetic materials. Curie constant (C) is related to the effective moments of a magnetic material at temperatures sufficiently high that the spin arrangement is random.

To confirm the magnetic behavior of these materials post-DFT Boltztrap technique [22] is utilized. The plots between χ and its inverse (χ^{-1}) versus temperature are plotted in Fig. 8 for $AOsO_3$ (A=Ca, Sr and Ba) compounds. The figure shows a decreasing trend of the susceptibilities with increasing temperature of the three compounds which are consistent with the experiments [13]. The appreciable decrease occurs in susceptibilities of the these compounds as we go from temperature range of 0–100 K, while this change goes further from 100 K to 250 K but is not as much as in the temperature range of 0 K to 100 K. The saturation in magnetic susceptibility will probably be observed beyond a temperature of 280 K. As far as the magnitude of the magnetic susceptibilities of the three compounds are concerned, χ for $CaOsO_3$ is 9.88 (10^{-3} emu mol^{-1}) at 25.47 K, for $SrOsO_3$ is 7.75 (10^{-3} emu mol^{-1}) at 24.62 K and for $BaOsO_3$ is

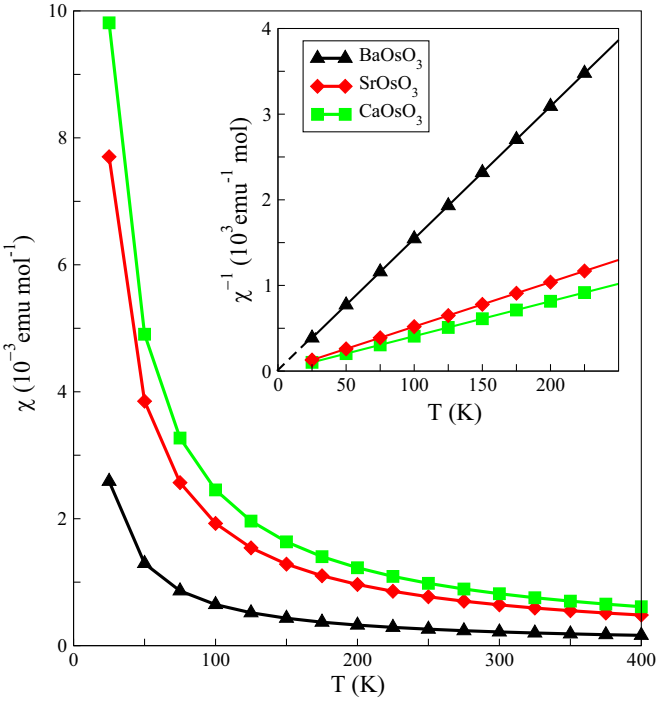

Fig. 8. Magnetic susceptibility versus Temperature of $AOSO_3$ (A=Ca, Sr and Ba).

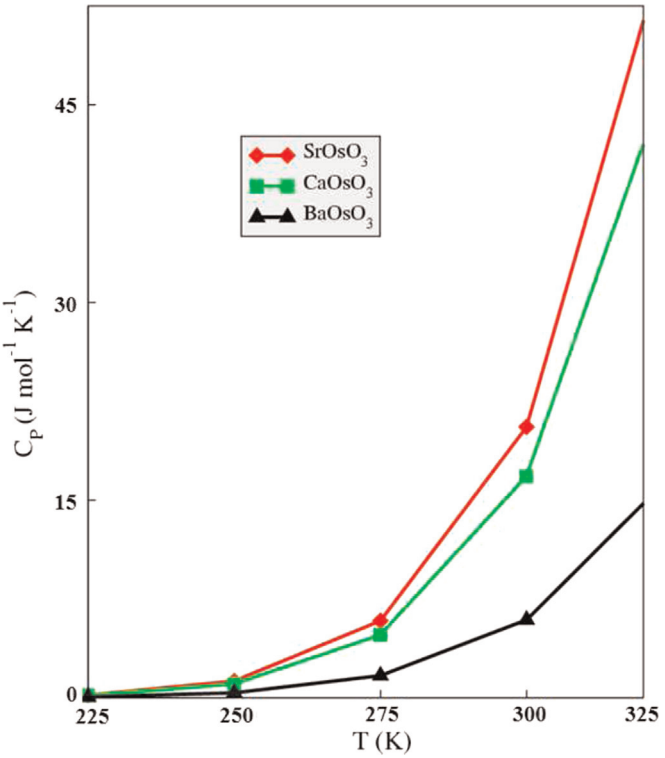

Fig. 9. Specific heat (C_p) versus Temperature of $AOSO_3$ (A=Ca, Sr and Ba).

2.71(10^{-3} emu mol^{-1}) at 23.77 K. Our magnetic susceptibility curves are also consistent with the experiments [13] in which these materials show no significant magnetization at very low temperature. The inverse plot of the magnetic susceptibility shows that Weiss constant (θ) is positive for $CaOsO_3$ and $SrOsO_3$ at about θ=25 K for both compounds, justifying Curie Weiss law of ferromagnetism. Furthermore, in the plot of $BaOsO_3$, $1/\chi$ versus T passes through the origin (θ=0 K), which confirms the paramagnetic nature of the compound.

Specific heat for the $AOsO_3$ compounds are also calculated using post-DFT treatment. Fig. 9 shows the heat capacity (C_p) versus temperature (T) plots for all the three compounds. The figure reveals that a slight increase is observed in C_p from 225 K to 250 K, while this change (increase) is noticeable as we proceed further in temperature axis from 250 K to 300 K and this trend goes on further in the same way justifying the direct proportionality relation in between C_p and T. Finally a stage reaches where phase transition occurs in these compounds. From the plot in Fig. 9, the observed values of C_p for the three compounds at room temperature (300 K) are, C_p for $CaOsO_3$, $SrOsO_3$ and $BaOsO_3$ are 20 J mol^{-1} K^{-1}, 23 J mol^{-1} $K^{-1}$and 6 J mol^{-1} K^{-1} and on further increasing the temperature the values of C_P increases, our results show that the molar heat capacity of $SrOsO_3$ is larger than those of the rest compounds and the trend is found to be consistent with the experiments.

4. Conclusions

In summary the structural properties and geometries, chemical bonding nature, cohesive energies and magneto-electronic properties of the perovskites $AOsO_3$ (A=Ca, Sr and Ba) have been theoretically investigated by DFT. Structural properties are calculated by DFT as well as by ionic radii methods and are found in close agreement with experiments. The electron densities in (100) and (110) plane of these compounds elaborate the bonding nature

among the different atoms. The cohesive energies are calculated to study the relative stability of these compounds. The electronic band structures reveal the metallic nature of these compounds. The optimized magnetic phase and BoltzTraP calculations confirm that $BaOsO_3$ is paramagnetic while $CaOsO_3$and $SrOsO_3$ are weak ferromagnetic in nature. The calculated magnetic moments of the stated compounds are also consistent with the experimental low temperature range. Furthermore the directional magnetic study shows that these compounds are magnetically anisotropic, and reveals that the easy magnetization axis is [001] direction.

References

[1] A.L. Marco, D. Haskel, N.S. Neto, J.C. Lang, V.V. Krishnamurthy, S. Chikara, G. Cao, M. van Veenendaal, Phys. Rev. Letts. 105 (216407) (2010) 1–4.
[2] K. Fujiwara, Y. Fukuma, J. Matsuno, H. Idzuchi, Y. Niimi, Y.C. Otani, H. Takagi, Nat. Commun. 4 (2893) (2013) 1–6.
[3] J. Igarashi, T. Nagao, J. Phys. Soc. Jpn. 83 (053709) (2014) 1–5.
[4] J. Igarashi, T. Nagao, Phys. Rev. B 88 (104406) (2013) 1–5.
[5] D. Pesin, L. Balents, Nat. Phys. 6 (2010) 376–381..
[6] H. Onishi, J. Phys.: Conf. Ser. 391 (012102) (2012) 1–4.
[7] S. Fujiyama, H. Ohsumi, K. Ohashi, D. Hirai, B.J. Kim, T. Arima, M. Takata, H. Takagi, Phys. Rev. Letts. 112 (016405) (2014) 1–5.
[8] X. Liu, V.M. Katukuri, L. Hozoi, W.G. Yin, M.P.M. Dean, M.H. Upton, J. Kim, D. Casa, A. Said, T. Gog, T.F. Qi, G. Cao, A.M. Tsvelik, J. van den Brink, J.P. Hill, Phys. Rev. Lett. 109 (157401) (2012) 1–5.
[9] B.J. Kim, H. Jin, S.J. Moon, J.Y. Kim, B.G. Park, C.S. Leem, J. Yu, T.W. Noh, C. Kim, S.J. Oh, J.H. Park, V. Durairaj, G. Cao, E. Rotenberg, Phys. Rev. Lett. 101 (076402) (2008) 1–4.
[10] B.J. Kim, H. Ohsumi, T. Komesu, S. Sakai, T. Morita, H. Takagi, T. Arima, Science 323 (2009) 1329–1332.
[11] C.Q. Jin, J.S. Zhou, J.B. Goodenough, Q.Q. Liu, J.G. Zhau, L.X. yang, Y. Yu, R.C. Yu, T. katsura, A. Shatsky, E. Ito, Proc. Nat. Acad. Sci. 105 (2008) 7115–7119.
[12] J.B. Goodenough, J.A. Kafalas, J.M. Longo, "High Pressure Synthesis" (P. Hagenmuller), Preparative Method in Solid State Chemistry, Academic Press, New York, 1972.
[13] Y. Shi, Y. guo, Y. Shirako, W. Yi, X. Wang, A.A. Belk, Y. Matsushita, H.L. Feng, Y. Tsujimoto, M. Arai, N. Wang, M. Akaogi, J. Am. Chem. Soc. 135 (44) (2013) 16507–16516.
[14] P. Zheng, Y.G. Shi, A.F. Fang, T. Dong, K. Yamaura, N.L. Wang, J. Phys.: Condens. Matter. 26 (435601) (2014) 1–5.
[15] M.C. Jung, K.W. Lee, Phys. Rev. B 90 (045120) (2014) 1–6.
[16] W. Kohn, L.J. Sham, Phys. Rev. 140 (4A) (1965) A1133–A1138.
[17] O.K. Andersen, Phys. Rev. B 12 (8) (1975) 3060–3083.
[18] J.P. Perdew, A. Ruzsinszky, G.J. Csonka, O.A. Vydrov, G.E. Scuseria, L. A. Constantin, X. Zhou, K. Burke, Phys. Rev. Lett. 100 (136406) (2008) 1–4.
[19] V.I. Anisimov, I.V. Solovyev, M.A. Korotin, Phys. Rev. B 48 (23) (1993) 16929–16934.
[20] K. Schwarz, J. Solid State Chem. 176 (2003) 319–328.
[21] P. Blaha, K. Schwarz, G.K.H. Madsen, D. Kvasnicka, J. Luitz, Wien2k: An augmented plane wave plus local orbitals program for calculating crystal properties, Vienna university of Technologsy, Austria, 2001.
[22] G.K.H. Madsen, D.J. Singh, Compute. Phys. Commun. 175 (2006) 67–71.
[23] P.B. Allen, W.W. Schulz, Phys. Rev. B 47 (1993) 14434–14439.
[24] F. Birch, Phys. Rev. 71 (11) (1947) 809–824.
[25] R. Ubic, G. Subodh, J. Alloys Compd. 488 (2009) 374–379.
[26] A.S. Verma, V.K. Jindal, J. Alloys Compd. 485 (2009) 514–518.
[27] Z. Ali, I. Ahmad, B. Amin, M. Maqbool, G. Murtaza, I. Khan, M.J. Akhtar, F. Ghaffor, Physica B 406 (2011) 3800–3804.
[28] J.B. Goodenogh, Rep. Prog. Phys. 67 (2004) 1915–1993.
[29] N. Xu, H. Zhao, X. Zhou, W. Wei, X. Lu, W. Ding, F. Li, Int. J. Hydrog. Energy 35 (2010) 7295–7301.
[30] Z. Li, T. Iitaka, T. Tohyama, Phys. Rev. B 86 (094422) (2012) 1–4.
[31] J.S. Zhou, K. Matsubayashi, Y. Uwatoko, C.Q. Jin, J.G. Cheng, J.B. Goodenough, Q. Q. Liu, T. Katsura, A. Shatskiy, E. Ito, Phys. Rev. Lett. 101 (077206) (2008) 1–4.
[32] R. Hoffman, Rev. Mod. Phys. 60 (3) (1988) 601–628.
[33] R. Gaudoin, W.M. Foulkes, G. Rajagopal, J. Phys.: Condens. Matter 14 (2002) 8787–8793.
[34] D.V. Suetin, V.V. Bannikov, I.R. Shein, A.L. Ivanovskii, Phys. Status Solidi B 246 (2009) 1646–1651.
[35] W.H. Qi, M.P. Wang, J. Mat. Sci. Lett. 21 (2002) 1743–1745.
[36] S. Blundell, "Magnetism in Condensed Matter", Oxford University Press, New York, 2001.
[37] C. Kittel, "Introduction to Solid State Physics", 8th Edition, Willey & Sons, New York, 2005.